

Fluorescent Nanoparticle Beacon for Logic Gate Operation Regulated by Strand Displacement

Jing Yang,^{*,†} Lingjing Shen,[‡] Jingjing Ma,[§] H. Inaki Schlaberg,[†] Shi Liu,[†] Jin Xu,[§] and Cheng Zhang^{*,§}

[†]School of Control and Computer Engineering, North China Electric Power University, Beijing 102206, China

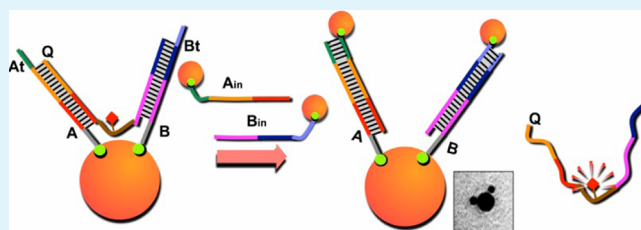
[‡]College of Life Science, Shannxi Normal University, Xi'an 710062, China

[§]Institute of Software, School of Electronics Engineering and Computer Science, Key Laboratory of High Confidence Software Technologies of Ministry of Education, Peking University, Beijing 100871, China

S Supporting Information

ABSTRACT: A mechanism is developed to construct a logic system by employing DNA/gold nanoparticle (AuNP) conjugates as a basic work unit, utilizing a fluorescent beacon probe to detect output signals. To implement the logic circuit, a self-assembly DNA structure is attached onto nanoparticles to form the fluorescent beacon. Moreover, assisted by regulation of multilevel strand displacement, cascaded logic gates are achieved. The computing results are detected by methods using fluorescent signals, gel electrophoresis and transmission electron microscope (TEM). This work is expected to demonstrate the feasibility of the cascaded logic system based on fluorescent nanoparticle beacons, suggesting applications in DNA computation and biotechnology.

KEYWORDS: fluorescent nanoparticle beacon, multilevel strand displacement, cascaded logic gate, TEM image, fluorescent signals, PAGE analysis



1. INTRODUCTION

In traditional silicon-based computers, logic gates perform all types of operations by receiving inputs representing true (high voltage) or false (low voltage), and then producing the corresponding electronic outputs.^{1,2} With the advancement of DNA computation and nanotechnology, nucleic acid, as a basic component, has attracted considerable attention in molecular logic systems because its unique features, involving the Watson–Crick base pairing, strand displacement, and its ability to conjugate certain target molecules such as nanoparticles (NPs),^{3–5} quantum dots,⁶ and proteins.⁷ Molecular logic gates can be built using deoxyribozymes,^{8,9} restriction enzymes,¹⁰ and other small molecules.^{11–13} Recently, the method of strand displacement has inspired the development of DNA circuits such as a scalable DNA circuit architecture,¹⁴ and enzyme-free hairpin assembly circuits.¹⁵ In particular, this idea has been demonstrated to be a capable computing system.¹⁶

On the other hand, previous researches have revealed that AuNPs have been widely applied in biological sciences because of their unique optoelectronic properties and excellent biocompatibility.^{17–22} Interestingly, upon theoretical predictions and experimental studies, AuNPs have been demonstrated as a kind of “super-quenchers”, effectively quenching a wide range of dyes.^{23–27} On the basis of this quenching effect, Dustin et al. constructed a self-assembled nanoparticle probe, in which fluorescent signals were regulated by adding input DNA strands.²⁸ In 2009, a type of gold-nanoparticle-based multicolor fluorescent nanobeacon was designed to simultaneously detect

adenosine, potassium ions, and cocaine with high selectivity.²⁹ In addition, employing molecular beacons (MBs), Shipng Song et al. developed a nanoMB that utilized special structures of hairpin DNA.³⁰ In these works, it should be noted that, (1) all resulting signals are induced by directly adding input molecules; (2) the DNA structures attaching onto AuNPs are rather simple, and each of them is just modified with one thiol-group.

In this study, we have designed a fluorescent nanoparticle beacon to implement logic gate operations regulated by two-level strand displacement. Different from previous work, this study has two characteristics: (1) the cascading two-level circuits. In the logic gate system, single-stranded DNA is used as the input signal to induce a series of controllable strand displacements, through which the displacing strands will be released. Subsequently, the fluorescent beacons will be triggered by the released DNA strands. (2) Self-assembly DNA structures attaching onto AuNPs. The fluorescent nanoparticle beacon is constructed based on a self-assembly DNA structure consisting of three single-stranded DNA molecules, two of which are thiolated. In the experiment, the logic operation result is detected by three methods: fluorescence detection, PAGE analysis, and TEM image.

Received: April 23, 2013

Accepted: June 4, 2013

Published: June 7, 2013

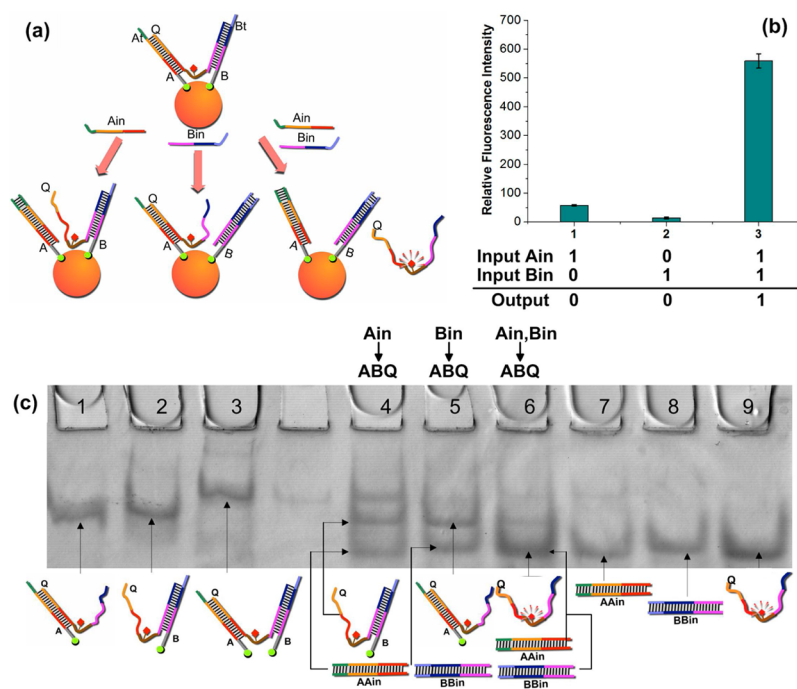


Figure 1. Basic molecular “AND” logic gate I. (a) Schematic illustration of the operational design of gate I. The DNA strands of the same color are complementary to each other. (b) Fluorescence intensity measured at 564 nm. The truth table refers to the fluorescence signal. (c) PAGE gel analysis of the basic logic gate. Lanes 1–3 and 7–9 correspond to different assembly polymers: A_Q, B_Q, AB_Q, AA_{in}, BB_{in}, and strand Q; lanes 4–6 correspond to the computation results of logic gate I. Error bars represent one standard deviation from triplicate analyses.

2. EXPERIMENTAL METHODS

Logic Gate Preparation. Logic gates were formed by mixing several kinds of DNA strands in a course of slow annealing. Various equimolar DNA strands were added to a final concentration of 3 μM , in 1 \times TAE/Mg²⁺ buffer (0.04 M Tris acetate, 1 mM EDTA, 12.5 mM Mg acetate, pH 8.3) or 0.5 \times TBE buffer (89 mM Tris, 89 mM boric acid, 2 mM EDTA, pH 8.0). The mixture is hybridized at the reaction condition of 37 $^{\circ}\text{C}$ for 2 h. In a two-layer “AND” logic gate, after first constructing each gate separately, the two-layer “AND” logic gate was then formed by mixing the solutions of all gates.

DNA/AuNP Preparation. The thiolated DNA strands were incubated with a specific ratio of AuNPs in 0.5 \times TBE buffer and a final concentration of 50 mM NaCl for 4 to 6 h at room temperature.³¹ After that, 3% agarose gel was used to separate DNA/AuNP conjugates with different discrete DNA bands for 1.5 h. The target bands of conjugates I, II, and III were run into a glass fiber filter membrane assisted by a dialysis membrane (MWCO 14000). Conjugate I consisted of one AuNP (15 nm) and a few copies of the nanostructure ABQ, while in conjugate II, a large number of copies of A_{in} (or B_{in}) were conjugated with one AuNP (5 nm). Similarly, in conjugate III, a large number of copies of the nanostructure ABQ were conjugated with one AuNP (15 nm). The DNA/AuNP conjugates were then collected in test tubes. Each sample of DNA/AuNP conjugate was quantified by optical absorbance at 520 nm, and preserved at 4 $^{\circ}\text{C}$.

Displacement of Input DNA Strands. Logic gates were displaced in 1 \times TAE/Mg²⁺ buffer, with a final concentration of 3 μM . Input DNA strands (at the same concentrations with gate strands) were added to a solution containing DNA gates and reacted for more than 5 h at room temperature. Next, the displaced products were stored at 4 $^{\circ}\text{C}$ for PAGE or fluorescence detection.

Displacement of DNA/AuNP Conjugates. Conjugates I and III were prepared by incubating 15 nm AuNPs and annealing products (the nanostructure ABQ) together overnight. Conjugate II was prepared by incubating 5 nm AuNPs and the thiolated ssDNA (A_{in}-SH or B_{in}-SH) together overnight. To implement displacement between conjugate I and conjugate II, DNA/AuNP conjugates A_{in}-SH or B_{in}-SH or both (0.3 μM) were added to the gate sample (0.27 μM) in a final volume of 20 μL for 10 h at room temperature.

Fluorescence Experiments. Each logic gate sample was diluted from 20 μL to a final volume of 100 μL for detection, with a 120 pmol gate strand and 240 pmol input strand. After adding input strands to react for 2 h or other specific intervals, the samples were excited at 550 nm, and the resulting fluorescent output signal was recorded with emission readings at 564 nm on a spectrophotometer (Hitachi F-2700). DNA displacements were carried out at room temperature, in 0.5 \times TBE buffer with a final NaCl concentration of 50 mM.

TEM Analysis. Purified DNA/AuNP conjugates were freshly isolated. A 3–6 μL droplet of the sample was deposited on carbon-coated grids (400 mesh, Ted Pella). The excess solution was then removed using a piece of filter paper. The grid was washed one to three times with Milli-Q water. TEM images were obtained using a Hitachi H-7650 transmission electron microscope.

3. RESULTS AND DISCUSSION

In our strategy, two logic systems were developed. (1) Gate I, a basic “AND” logic gate consisting of fluorescent nanoparticle beacons; (2) gates II and III, logic gates based on linear DNA strand displacement. The output strands from upstream gates served as input signals to trigger the downstream logic gate.

Gate I was constructed with strands A, B, Q and a 15 nm AuNP (Figure 1a). Each strand (see the Supporting

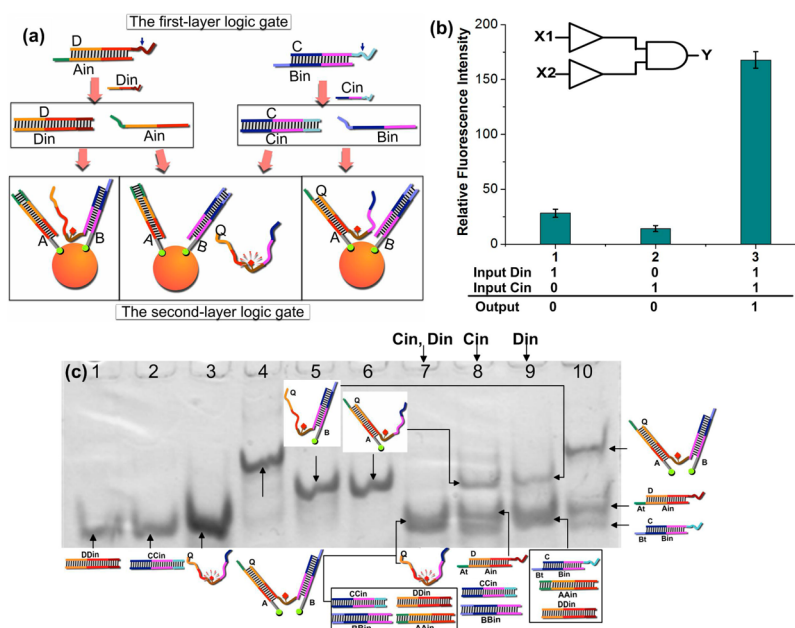


Figure 2. Two-layer molecular logic gate II consists of two “YES” gates and one “AND” gate. (a) Schematic illustration of the operational design of gate II. (b) The fluorescence experiment results. (c) PAGE gel analysis. Lanes 1–6 correspond to different assembly polymers DD_{in} , CC_{in} , Q , ABQ , BQ , and AQ , respectively; lanes 7 to 9 correspond to the computing results; lane 10 corresponds to the gate strands. Error bars represent one standard deviation from triplicate analyses.

Information, Table S1) was designed to test this gate. First, strands A, B, and Q (modified with the fluorophore Cy3 in the middle) were hybridized to yield a DNA self-assembly structure based on Watson–Crick base pairing. Next, the nanostructures were connected with 15 nm AuNPs via thiol groups to form fluorescent nanoparticle beacons, which served as a basic “AND” gate. In this logic system, the fluorophores were quenched in proximity to AuNPs. However, when strand Q was displaced and separated from strands A and B, the fluorescence intensity would be restored rapidly due to the separation of fluorophore and AuNP (Figure 1a). A true output of 1 is obtained only when both of the inputs are held at 1. In absence of adding input signals, no fluorescence signal was produced.

In the computing course of gate I, we used strands A_{in} and B_{in} as the two input strands. The computation was implemented by adding specific input strands to the gate solutions in three ways. First, addition of input strand A_{in} displaced only a partial region of strand Q by specifically recognizing the toehold of strand A. No significant fluorescent signal was produced because no separation happened between fluorophores and AuNPs (Figure 1b, L1). Moreover, if input strand B_{in} was added, strand Q_2 was gradually displaced. However, strand Q still attached onto AuNPs by hybridization with strand A, and no significant fluorescence was restored (Figure 1b, L2). Therefore, adding either A_{in} or B_{in} input strands did not result in a great increase of fluorescence intensity. Second, DNA strands A_{in} and B_{in} were added to gate I at the same time. After that, strands A_{in} and B_{in} completely released strand Q, and a significant fluorescent signal was observed because of the spatial separation of the fluorophore from the AuNP (Figure 1b, L3). In the experiment, it should be noted that there were still some fluorescent leakages produced in the reaction, because of cross-talk between signal strands.

Additionally, native PAGE results were used to detect the results of the basic logical computation. By strand displacement, it would produce output strands when adding either input

strands A_{in} , or B_{in} or both of them. As expected, strand Q was completely released in lane 6 (Figure 1c) only from input state (1, 1), but not from (1, 0) or (0, 1) input states. As shown in lanes 4 and 5, strand Q was only partially released, because either of the two inputs was held at 1. The experimental results demonstrated the proper execution of gate I at the molecular level.

To verify the feasibility of the regulating fluorescent nanoparticle beacon gate by strand displacement, we established a two-layer logic gate II, in which two “YES” gates and one gate I were cascaded with two-inputs (Figure 2a). Here, two upstream “YES” gates first produced output signal strands, which would induce the downstream “AND” gate. Initially, when two first-layer input strands D_{in} and C_{in} bound to the toeholds of two “YES” gates, output strands A_{in} and B_{in} were generated, respectively, serving as the second inputs for the downstream “AND” gate. In addition, two waste products DD_{in} and CC_{in} were also produced during the strand branch migration. For the downstream “AND” gate, the true result could be obtained only if both strands A_{in} and B_{in} from the upstream gate were present.

At first, the solution of gate II consisted of two substrates $A_{in}D$, $B_{in}C$ and the fluorescent beacon. The above computation could be implemented in three ways (Figure 2a). (1) When strand D_{in} was added to the solution of gate II, it gradually displaced strand A_{in} by recognizing the toehold of strand D. Next, the released output strand A_{in} triggered the downstream “AND” gate, and no significant fluorescent signal was produced (Figure 2b, L1). (2) Adding strand C_{in} (recognizing the toehold of strand C), strand B_{in} was released as an input to trigger the downstream logic gate. In this process, there also was no significant fluorescent signal (Figure 2b, L2). (3) Finally, when both inputs C_{in} and D_{in} were added, the output strands A_{in} and B_{in} were produced, and triggered the downstream gate simultaneously. Therefore, a significant fluorescent signal was restored (Figure 2b, L3).

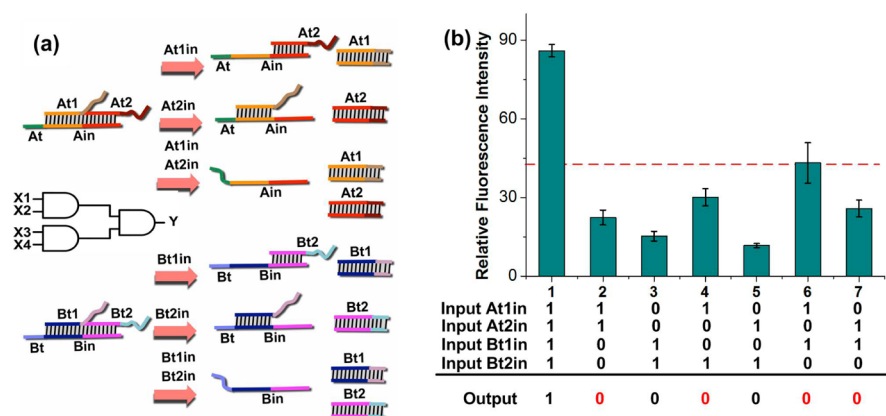


Figure 3. Two-layer molecular logic gate III consists of three “AND” gates. (a) Schematic illustration of the operational design of gate III. (b) Fluorescence experiment results. Error bars represent one standard deviation from triplicate analyses.

Here, the fluorescent detection result of logic gate II was further determined by PAGE analysis. Adding strand D_{in}, the displacement products were DD_{in}, AA_{in}, and BQ (Figure 2c, lane 9), and strand Q was not released. When adding strand C_{in}, strand Q had still not been released (Figure 2c, lane 8). When finally both the inputs C_{in} and D_{in} were added, strand Q was completely released (Lane 7). It is easy to see that the PAGE gel results are in accordance with fluorescence detection results.

To demonstrate scalability and modularity, three logic “AND” gates were cascaded into a circuit as another two-layer logic gate III. The circuit accepted four inputs: (At1_{in}, At2_{in}) and (Bt1_{in}, Bt2_{in}) in the first layer, and produced two outputs: A_{in} and B_{in}, respectively, used as the two inputs for the second layer (Figure 3a). From the experimental results, the additions of either (At1_{in}, At2_{in}) or (Bt1_{in}, Bt2_{in}) were not able to induce a significant fluorescent signal (Figure 3b, L2 and L3), and this was also proved by PAGE gel analysis (see Figure S8a in the Supporting Information). Moreover, when four inputs At1_{in}, Bt1_{in}, At2_{in}, and Bt2_{in} were added at the same time, the released output strands A_{in} and B_{in} completely displaced strand Q from the fluorescent nanoparticle beacon (see Figure S8a in the Supporting Information, lane 3). Therefore, a significant fluorescence signal was observed as expected (Figure 3b, L1). In a similar way, four further combinations of input strands were applied to this circuit (Figure S8b). Interestingly, in principle, only when adding all four inputs At1_{in}, Bt1_{in}, At2_{in}, and Bt2_{in}, would strands A_{in} and B_{in} be released. However, in the experiment, when adding any two of the four input strands, undesirable fluorescent leakages were produced (Figure 3b). Apparently, after displacement with input strands, the newly exposed regions of strands A_{in} and B_{in} would make their toeholds (At1 and Bt1) more active, and then increase the possibility of triggering downstream gates. In particular, the leakage produced when adding strands At1_{in} and Bt1_{in} was much larger than that when adding other input combinations (Figure 3b, L6). The possible reason may be that, newly exposed regions caused by adding strands At1_{in} and Bt1_{in} were rather closer to the toehold regions At and Bt, than those when adding other input combinations. Additionally, more control experiments were carried out by adding all combinations of three out of four strands into logic gate III (see the Supporting Information, Figure S9).

In this experiment, the assembly structures of AuNPs were utilized to further probe the results of gate I. In the reactions,

one 15 nm conjugate I was hybridized with 5 nm conjugate II either A_{in} or B_{in}, or both of them (Figure 4). By TEM

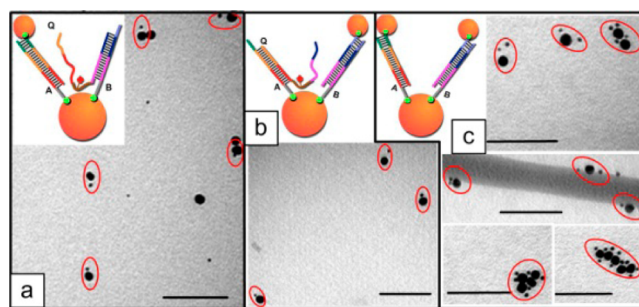


Figure 4. (a, b) Molecular geometry of AuNPs dimers was visualized by TEM with conjugate A_{in} and B_{in}, respectively; (c) TEM images were visualized with addition of both conjugates A_{in} and B_{in}. Scale bar: 100 nm.

detection, the obtained AuNPs clusters were dimers and trimers as expected, since the specific products were purified from the electrophoresis gel. In addition, we observed a number of other undesired AuNPs structures in the experiments. This phenomenon may result from the following reasons: 1) drying effect on TEM grids; 2) incomplete band separation; 3) a structural shelter (small nanoparticles may be shaded from an electron beam); 4) different picture angles of the TEM; 5) manual operations in purifying the fractions from gels.

4. CONCLUSION

In summary, we have developed a mechanism that utilizes controllable strand displacement to implement two-layer logic gates based on fluorescent nanoparticle beacons. The main motivations of this study are not only focused on constructing fluorescent nanoparticle beacons via complex DNA assembly structures, but also on establishing a controllably cascading molecular detecting system. By employing self-assembly DNA/AuNP conjugates as a basic work unit, the basic logic gate I operation is performed, wherein the computing results are readily detected by three methods of fluorescent signals, PAGE gel analysis and TEM image. Moreover, assisted by multilevel strand displacement, two-layer cascading logic circuits II and III are established, consisting of linear DNA strands gates (upstream) and the basic “AND” logic gate (downstream). Finally, the method of assembling AuNPs clusters is introduced

to provide direct evidence of the formation of nanoparticle beacon structures.

Although DNA sequences were carefully designed in this work, there still were some deficiencies generated during the experimental operations. In particular, leakages were observed in the course of multilevel gate operations. The probable reason may stem from complex regulating relationships between cascading levels, in which the exposed toehold regions play a critical role. Therefore, the DNA design should be improved in future research. This work is expected to provide researchers with an experimental basis for additional complex logic gate designs at the molecular level. It may also contribute to the advancement of molecular computation and DNA nanotechnology.

■ ASSOCIATED CONTENT

Supporting Information

Materials, experimental methods, and additional experimental data. This material is available free of charge via the Internet at <http://pubs.acs.org>.

■ AUTHOR INFORMATION

Corresponding Author

*E-mail: yangjing369@gmail.com (J.Y.); zhangcheng369@pku.edu.cn (C.Z.). Tel & Fax: +86-10-61771050.

Notes

The authors declare no competing financial interest.

■ ACKNOWLEDGMENTS

This research is supported by National Natural Science Foundation of China (Grants 61143003, 61272161, 61127005, 61133010), Programme of Introducing Talents of Discipline to Universities (B13009), the program for Changjiang Scholars and Innovative Research Team in University (IRT0952), and Fundamental Research Funds for the Central University (13QN14).

■ REFERENCES

- (1) Bi, S.; Yan, Y. M.; Hao, S. Y.; Zhang, S. S. *Angew. Chem., Int. Ed.* **2010**, *49*, 4438–4442.
- (2) Frezza, B. M.; Cockroft, S. L.; Ghadiri, M. R. *J. Am. Chem. Soc.* **2007**, *129*, 14875–14879.
- (3) Wen, Y.; Chen, L.; Wang, W.; Xu, L.; Du, H.; Zhang, Z.; Zhang, X.; Song, Y. *Chem. Commun.* **2012**, *48*, 3963–3965.
- (4) Claridge, S. A.; Liang, H. W.; Basu, S. R.; Frèchet, J. M. J.; Alivisatos, A. P. *Nano Lett.* **2008**, *8*, 1202–1206.
- (5) Sharma, J.; Chhabra, R.; Andersen, C. S.; Gothelf, K. V.; Yan, H.; Liu, Y. *J. Am. Chem. Soc.* **2008**, *130*, 7820–7821.
- (6) Schroedter, A.; Weller, H.; Eritja, R.; Ford, W. E.; Wessels, J. M. *Nano Lett.* **2002**, *2*, 1363–1367.
- (7) Satoshi, H.; Riho, G.; Tomohiro, S.; Shoji, T.; Kazuo, S. *Nano Lett.* **2009**, *9*, 2407–2413.
- (8) Stojanovic, M. N.; Stefanovic, D. *Nat. Biotechnol.* **2003**, *21*, 1069–1074.
- (9) Elbaz, J.; Lioubashevski, O.; Wang, F.; Remacle, F.; Levine, R. D.; Willner, I. *Nat. Nanotechnol.* **2010**, *5*, 417–422.
- (10) Benenson, Y.; Gil, B.; Ben-Dor, U.; Adar, R.; Shapiro, E. *Nature* **2004**, *429*, 423–429.
- (11) Privman, M.; Tam, T. K.; Pita, M.; Katz, E. *J. Am. Chem. Soc.* **2009**, *131*, 1314–1321.
- (12) Mu, L.; Shi, W.; She, G.; Chang, J. C.; Lee, S. T. *Angew. Chem., Int. Ed.* **2009**, *48*, 3469–3472.
- (13) Amir, L.; Tam, T. K.; Pita, M.; Meijler, M. M.; Alfonta, L.; Katz, E. *J. Am. Chem. Soc.* **2009**, *131*, 826–832.
- (14) Qian, L.; Winfree, E. *Science* **2011**, *332*, 1196–1201.

- (15) Li, B.; Jiang, Y.; Chen, X.; Ellington, A. D. *J. Am. Chem. Soc.* **2012**, *134*, 13918–13921.
- (16) Seelig, G.; Soloveichik, D.; Zhang, D. Y.; Winfree, E. *Science* **2006**, *314*, 1585–1588.
- (17) Cao, Y. C.; Jin, R.; Mirkin, C. A. *Science* **2002**, *297*, 1536–1540.
- (18) Rosi, N. L.; Mirkin, C. A. *Chem. Rev.* **2005**, *105*, 1547–1562.
- (19) Li, H.; Rothberg, L. J. *J. Am. Chem. Soc.* **2004**, *126*, 10958–10961.
- (20) Zhang, J.; Song, S.; Wang, L.; Pan, D.; Fan, C. *Nat. Protoc.* **2007**, *2*, 2888–2895.
- (21) Zhang, J.; Wang, L.; Pan, D.; Song, S.; Boyer, F. Y.; Zhang, H.; Fan, C. *Small* **2008**, *4*, 1196–1200.
- (22) Liu, J.; Lu, Y. *Angew. Chem., Int. Ed.* **2005**, *118*, 96–100.
- (23) Das, P. C.; Puri, A. *Phys. Rev. B* **2002**, *65*, 155416–155418.
- (24) Dulkeith, E.; Morteaux, A. C.; Niedereichholz, T.; Klar, T. A.; Feldmann, J.; Levi, S. A.; van Veggel, F.; Reinhoudt, D. N.; Möller, M.; Gittins, D. I. *Phys. Rev. Lett.* **2002**, *89*, 203002–203005.
- (25) Fan, C.; Wang, S.; Hong, J. W.; Bazan, G. C.; Plaxco, K. W.; Heeger, A. J. *Proc. Natl. Acad. Sci.* **2003**, *100*, 6297–6301.
- (26) Yun, C. S.; Javier, A.; Jennings, T.; Fisher, M.; Hira, S.; Peterson, S.; Hopkins, B.; Reich, N. O.; Strouse, G. F. *J. Am. Chem. Soc.* **2005**, *127*, 3115–3119.
- (27) Dulkeith, E.; Ringler, M.; Klar, T. A.; Feldmann, J.; Javier, A. M.; Parak, W. J. *Nano Lett.* **2005**, *5*, 585–589.
- (28) Maxwell, D. J.; Taylor, J. R.; Nie, S. J. *J. Am. Chem. Soc.* **2002**, *124*, 9606–9612.
- (29) Zhang, J.; Wang, L.; Zhang, H.; Boey, F.; Song, S.; Fan, C. *Small* **2009**, *6*, 201–204.
- (30) Song, S.; Liang, Z.; Zhang, J.; Wang, L.; Li, G.; Fan, C. *Angew. Chem., Int. Ed.* **2009**, *48*, 8670–8674.
- (31) Zanchet, D.; Micheel, C. M.; Parak, W. J.; Gerion, D.; Alivisatos, A. P. *Nano Lett.* **2001**, *1*, 32–35.